Engineering PMMA/PVA Polymer Blends with TiO_2-GO Nanofillers for Enhanced Structural and Optical Properties

Sunita Verma[1*], *Neha* Sharma[1], *S. Z.* Hashmi[2], *B. L.* Choudhary[1], *M. Ayaz* Ahmad[3] and *P. A.* Alvi[1*]

[1]Department of Physical Sciences, Banasthali Vidyapith, Banasthali-304022, Rajasthan, India
[2]Department of Chemistry, Banasthali Vidyapith, Banasthali-304022, Rajasthan, India
[3]Department of Mathematics, Physics and Statistics, Faculty of Natural Sciences, University of Guyana, P.O. Box 101110, Georgetown, Guyana

Abstract. For the first time, we present an overview of the structural and optical features of the newly formulated "PMMA-PVA-TiO_2-GO" polymer nanocomposites taking into account the polymer blend of PMMA and PVA matrix, while TiO_2 and GO are used as nanofillers in making the nanocomposite. The X-ray diffractometer (XRD) was employed to determine the structural characteristics of the samples, and a UV-Vis-NIR spectrometer was used to record the behaviour of optical absorbance. The nanocomposites were synthesized using a simple solution mixing method, ensuring uniform dispersion of nanofillers within the host polymer blend. XRD results confirms a reduction in crystallite size (from ~15 nm to ~11 nm), along with an increase in micro-strain and dislocation density, indicating increased lattice distortion and strong interfacial interactions. Mechanical parameters reveal significant improvements in Young's modulus and energy density with reduced flexibility reflecting a trade-off between stiffness and flexibility. Finding of spectrophotometer confirms a red shift in the absorption edge from 244 nm to 250 nm with enhanced UV absorption, while the optical bandgap remains nearly unchanged. In view of above analysis, these nanocomposites are suitable for advanced optoelectronic and structural applications.

1. Introduction

Polymer nanocomposites (PNCs) have come out as a promising alternative to conventionally filled polymers. Nanometre scaled fillers are used in these materials which allows for their uniform dispersion within the polymer matrix. Polymer nanocomposites are advanced materials consisting of a polymer matrix reinforced with nanofillers (at least one dimension <100nm). When compared to traditional polymer composites, improved filler dispersion and enhanced interfacial interactions lead to superior mechanical, thermal, electrical, optical, and barrier properties at low filler loading as they combine high aspect ratio fillers like carbon

* Corresponding author: drpaalvi@gmail.com

nanotubes, nanoclays, or graphene within polymers to enhance performance over conventional composites [1-4].

Over the last few years, polymer nanocomposites have drawn significant attention due to their exceptional performance and their ability to alter properties by adjusting the type and concentration of nanomaterials or nanofillers integrated into lightweight and natural polymer matrices [5-7]. The size of nanoparticles ranges from 1 to 100 nm. They exhibit unique atomic level characteristics on this scale which makes them valuable for a wide range of applications. Nanofillers are defined as additives with at least one dimension below 100 nm, and their effectiveness arises from their high specific surface area. The incorporation of nanofillers enhances optical transparency, ultraviolet shielding, electrical conductivity, and dielectric properties, making polymer nanocomposites suitable for advanced applications such as sensors, electronics, optoelectronics, and energy storage devices. There are various types of nanoparticles remain which includes metallic nanoparticles, non-metallic and ceramic nanoparticles, semiconductor nanoparticles, and carbon-based nanoparticles. The development of advanced functional nanocomposites generally involves combination of inorganic crystals with organic molecules, as single component materials rarely achieve the desired multifunctional performance. Organic –inorganic hybrid polymer nanocomposites provide improved and tuneable properties due to the complementary characteristics of both organic and inorganic phases [8, 9]. However, achieving seamless integration of these phases particularly through polymerization remain challenging because of the fundamentally different formation mechanisms of organic and inorganic structures. Several approaches have been explored to fabricate organic-inorganic hybrid polymers, among which solution blending is a simple and widely used technique [10, 11]. In this method, the organic polymer is first synthesized in solution, followed by the incorporation of the inorganic component.

Based on dimensionality, Nanofillers can be categorised as zero-dimensional, one-dimensional two-dimensional (2D), and three-dimensional (3D) types. One-dimensional nanofillers be composed of nanofibers, nanotubes, and nanowires, whereas two-dimensional nanofillers involve graphene, reduced graphene oxide (rGO), and graphene oxide (GO). Three-dimensional nanofillers involve spherical and cubical nanoparticles. Carbon based nanofillers, specifically graphene, GO [12] and rGO [13] and carbon nanotubes [14], due to their high mechanical strength and large aspect ratios demonstrate exceptional properties.

In this article, two different nanofillers i.e., GO sheets and TiO_2 nanoparticles were added to the "PMMA-PVA-TiO_2-GO" polymer nanocomposites. The addition of two different nanofillers in PMMA-PVA-TiO_2-GO polymer nanocomposites shows a synergistic effect that enhances structural, optical, mechanical, and electrical properties more effectively than a single filler system. In fact, the TiO_2 nanoparticles improves thermal stability and photocatalytic behaviour, while GO enhances interfacial interaction, mechanical strength, and charge transport within the polymer matrix.

2. Sample preparation: Experimental detail

To synthesize the composite samples of PMMA/PVA/TiO_2/GO combination, an easy route i.e., simple mixing route was adopted. At initial stage, the uniform solutions of PVA and PMMA were prepared via dissolving in suitable solvent such as DMSO (dimethyl sulfoxide). While the nanofillers TiO_2 and GO were dispersed in same solvent like DMSO using ultra-sonication treatment. Both the dispersed nanofillers mixed with each other and the resulting product was added into the solution of PVA and PMMA as obtained earlier. The final solution of PVA, PMMA, TiO_2 and GO was kept on magnetic stirrer for 4 hours at temperature ~ 80

^{0}C. The magnetic stirrer treatment was given to the solution for making it homogeneous. The well-dispersed final solution was then cast onto Teflon plate and allowed to dry, during which solvent evaporation occurs, leading to the formation of a solid, free-standing PMMA/PVA/TiO_2/GO nanocomposite film. The Figure 1 shows the sequential steps to prepare the PMMA/PVA/TiO_2/GO polymer nanocomposites.

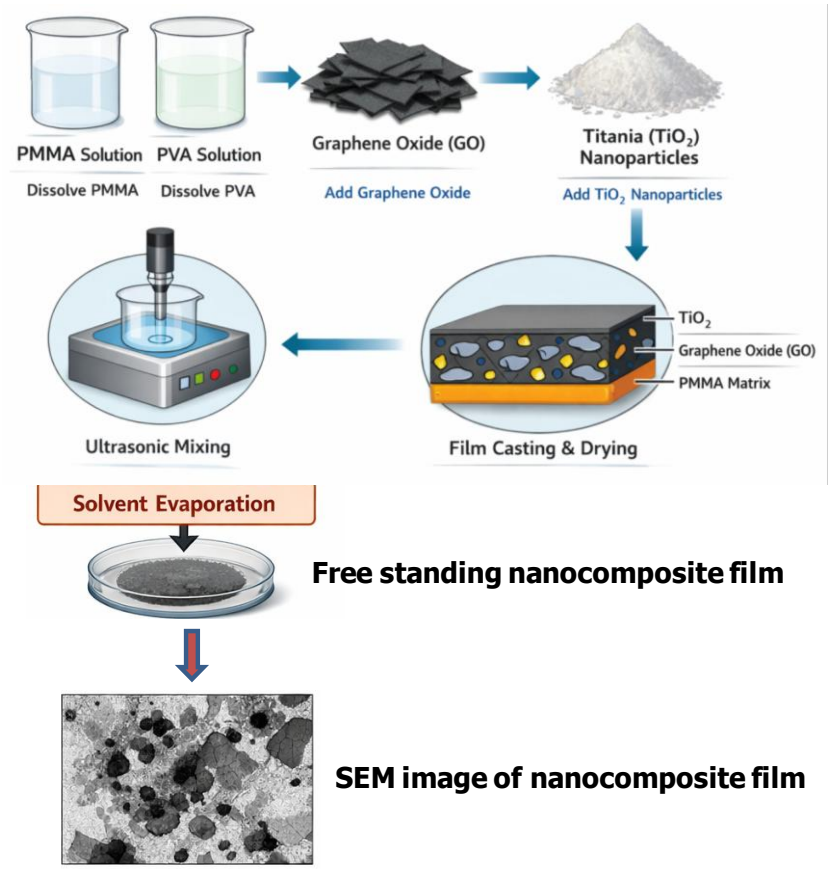

Fig. 1. Steps involved in preparation of PMMA-PVA-TiO_2-GO polymer nanocomposites

3. Characterization results and their analysis

To investigate the structural aspects of PMMA-PVA-TiO_2-GO polymer nanocomposites, X-ray diffractometer (Bruker-D8 Advance, with Cu-Ka radiation with wavelength~1.5406 Å) was brought in use. The recorded X-ray diffraction (XRD) patterns of pure PMMA/PVA polymer blends and PMMA-PVA-TiO_2-GO polymer nanocomposites are shown in Figure 2(a, b). The XRD patterns of pure PMMA/PVA blend a broad diffraction peak is observed at around 19° - 22°, as shown in Figure 2(a). This broad hump shows the amorphous nature of the polymeric blend. PMMA and PVA both are natural predominantly amorphous polymers, and their blending results in a semi-crystalline structure with low crystallinity, which is distinctive for polymeric systems including PVA and PMMA. Refer to Figure 2(b), the XRD patterns of PMMA/PVA/GO/TiO_2 nanocomposites that significant structural changes are observed after the incorporation of nanofillers TiO_2 and graphene oxide (GO). Upon

incorporation of GO and TiO_2, the XRD pattern shows sharp and intense diffraction peaks present at ~ 25°, 38°, 48°, 54°, and 62°, corresponding to crystalline planes of TiO_2 validating its successful incorporation into the polymer matrix. These peaks are normally matched well with the standard JCPDS (joint committee on powder diffraction standards) data, suggesting the presence of anatase or rutile phases [15]. Further addition of graphene oxide (GO) filler leads to slight peak shifting and broadening in the XRD pattern. This behaviour suggested strong interfacial interaction between the polymer chains and nanofillers, which influence the ordering of polymer chains. The decrease in peak intensity and increase in peak width indicates a reduction in crystallinity due to the interruption of the regular polymer structure by TiO_2 and GO nanoparticles. The decrease in intensity and slight shift of the polymer hump indicates strong interfacial interaction between polymer chains and nanofillers. GO enhances dispersion and induces partial ordering, resulting in a semi-crystalline structure.

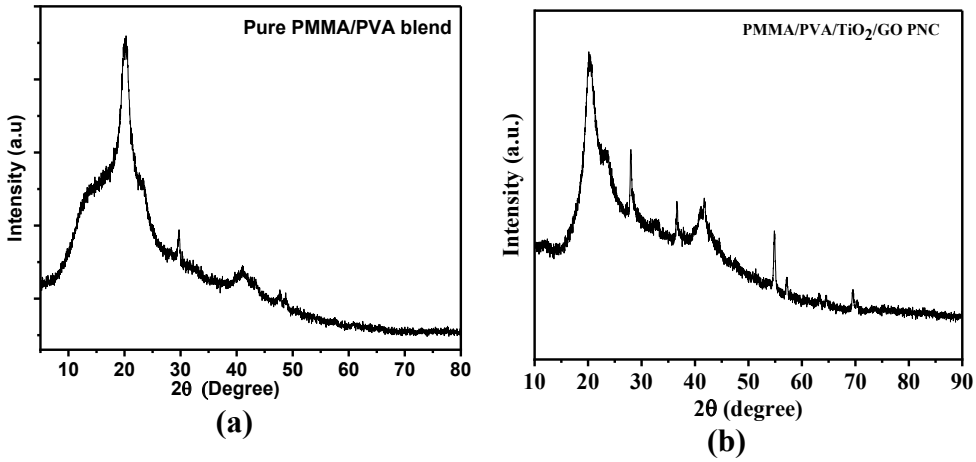

Fig. 2. XRD spectra of (a) Pure PMMA/PVA blend (b) PMMA-PVA-TiO_2-GO polymer nanocomposites

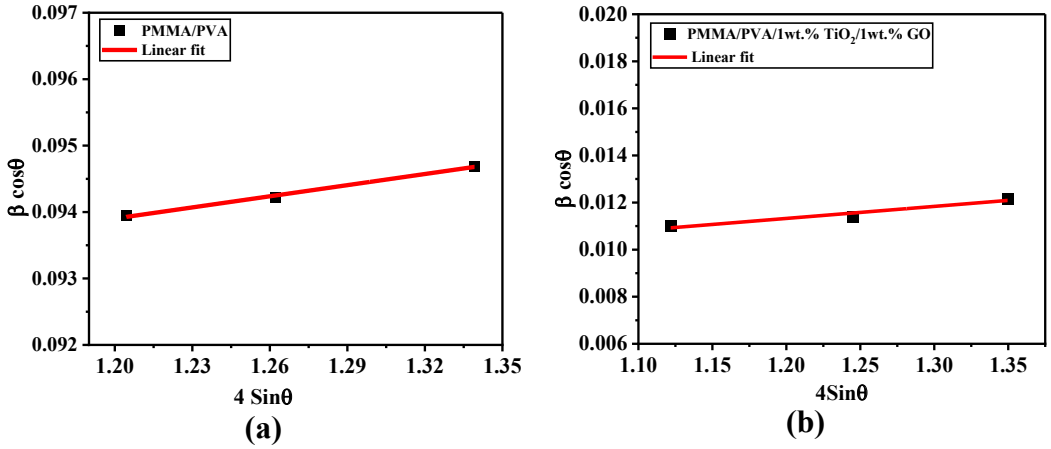

Fig. 3. W-H plots for (a) Pure PMMA/PVA blend (b) PMMA-PVA-TiO_2-GO polymer nanocomposites

From the XRD data, the structural parameters like crystallite size, micro-strain, and dislocation density of the prepared polymer nanocomposites. For calculating the crystallite size (D), the Scherrer equation, as given below, was used:

$$D = K\lambda/(\beta\cos\theta) \quad (1)$$

where D = crystallite size (nm), K = shape factor (≈ 0.9), λ = X-ray wavelength (Cu-Kα = 0.15406 nm), β = FWHM (in radians), θ = Bragg angle.

The numerical values of calculated crystallite size (D) are mentioned in Table 1. In addition, the micro-strain (ε) exiting in the composite samples were also calculated using W-H relation, as given below:

$$B\cos\theta = (K\lambda/D) + (4 \times \varepsilon\sin\theta) \quad (2)$$

where D is crystallite size (calculated from Scherrer relation), θ represents Bragg angle, ε represents micro-strain. For the PMMA/PVA blends and PMMA-PVA-TiO_2-GO polymer nanocomposites, the W-H relation has been plotted between βcosθ vs 4sinθ and shown in Figure 3(a, b). From Figure 3(a, b), one can extract the slope that represents micro-strain ε. The micro-strain in the polymer nanocomposites arises due to internal stress and structural mismatches at the microscopic level. Additionally, agglomeration of nanofillers and processing conditions may also be the possible causes.

Another structural parameter is dislocation density that arises due to structural irregularities introduced during processing and the presence of nanofillers incorporated into the polymer matrix. The dislocation density (δ) in the composite samples can be estimated by using the expression: $\delta=1/D^2$. The numerical values of the calculated δ for the composite samples are mentioned in table 1. Furthermore, the mechanical parameters like energy density, Young's modulus and flexibility have also been studied with the help of XRD data recorded from X-ray diffractometer. For these mechanical parameters, the following expression can be used for Young's Modulus (Y): $Y = \sigma/\varepsilon$, for Energy Density (u): $u = \sigma\varepsilon / 2$, for flexibility, $f = 1/Y$ where, σ and ε are the stress and micro-strain respectively. All these mechanical parameters i.e. energy density, Young's modulus and flexibility have been calculated and mentioned in Table 1. Referring to Table 1, the numerical values of structural and mechanical parameters show that addition of GO/TiO_2 nanofillers to the PMMA/PVA polymer blend alters both structural and mechanical properties. The crystallite size reduces from ~15 nm to ~11 nm, indicating fine structural domains, while the micro-strain (from 0.02219 to 0.02386) and dislocation density (from 0.00426 nm^{-2} to 0.00794 nm^{-2}) increase, suggesting more lattice distortion and defects due to the nanofillers incorporation. From the perspective of mechanical features, the prepared polymer nanocomposite becomes significantly stronger and stiffer, as seen from the rise in stress (from 4.525 to 8.165) and Young's modulus (from 2.015 to 4.631 GPa), along with an increase in energy density (from 13.316 kJ/m^3 to 15.435 kJ/m^3), indicating improvement in load-bearing and energy storing capability. Nevertheless, flexibility of the nanocomposite material reduces significantly (from 0.49628 to 0.21593), that reflects a trade-off where improved mechanical strength and stiffness comes at the cost of reduced flexibility.

For investigating the optical features, the UV-Vis-NIR spectrophotometer was used. Initially, by using the spectrophotometer the optical absorbance spectra was recorded. The recorded absorbance spectra of the PMMA-PVA polymer blends and PMMA-PVA-TiO_2-GO polymer nanocomposites have been shown in Figure 4(a, b). Refer to Figure 4, the absorbance spectra falling within the UV-Vis region show that the PMMA-PVA polymer blend exhibits a strong absorption edge ~ 244 nm, while the polymer nanocomposite (PMMA-PVA-TiO_2-GO) shows a slight red shift to ~ 250 nm along with enhanced absorbance in the UV region. This alteration in absorbance spectra indicates improvement in light-matter interaction due to the presence of TiO_2 and GO nanofillers. Moreover, this shift in in absorbance spectra suggests

modifications in the electronic structure and increased number of defect levels introduced by GO and TiO_2 nanofillers incorporated into the polymer blend.

Table 1. Structural and optical parameters of PMMA-PVA-TiO_2-GO polymer nanocomposites

S. No.	Structural/ optical parameters	Sample specifications	
		Pure PMMA/PVA	**PMMA/PVA/ 1wt.% (GO+TiO_2)**
1.	Crystallite size, D (nm)	~ 15	~ 11
2.	Micro-strain (ε)	0.02219	0.02386
3.	Dislocation density, δ (nm^{-2})	0.00426	0.00794
4.	Stress(S)	4.525	8.165
5.	Young's Modulus (Y) GPa	2.015	4.631
6.	Energy Density KJ/m^3	13.316	15.435
7.	Flexibility	0.49628	0.21593
8.	Optical band edge (nm)	244	250
9.	Optical band gap (eV)	5.25	5.26

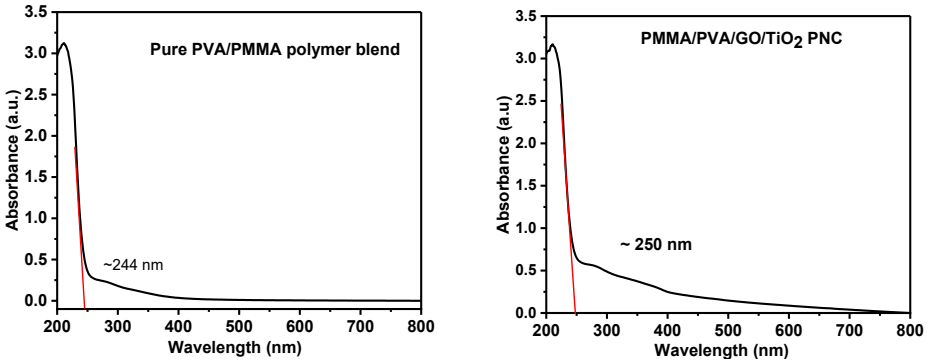

(a) **(b)**

Fig. 4. Absorbance spectra of (a) Pure PMMA/PVA blend (b) PMMA-PVA-TiO_2-GO polymer nanocomposites

The recorded spectra were used to study the Tauc's plot which his helpful in estimating the other optical parameters like optical bandgap, refractive index and metallic criteria of the prepared nanocomposites. The Tauc's plot for the PMMA-PVA polymer blends and PMMA-PVA-TiO_2-GO polymer nanocomposites have been shown in Figure 5 (a, b). For plotting the Tauc's plots, the following relation was used [16-18]:

$$(\alpha h\nu)^n = C(h\nu - E_g) \quad (3)$$

For calculating the direct bandgap, the index $n = 2$ should be considered, while C is an arbitrary constant, and α is optical absorption coefficient which was calculated using the relation $\alpha = 2.303\ A/t$, where A and t are absorbance and film thickness, respectively.

Figure 5 presents Tauc's plots used to estimate the direct optical bandgap of the PMMA-PVA polymer blends and PMMA-PVA-TiO*2*-GO polymer nanocomposites, where both materials exhibit almost equal bandgap values, with a slight increase, as mentioned in the Table 1. This marginal change indicates that while the nanofillers affect the absorption behaviour and optical transitions, they do not drastically alter the fundamental band structure or optical bandgap, but instead contribute to subtle electronic interactions and improved optical behaviour of the polymer nanocomposite.

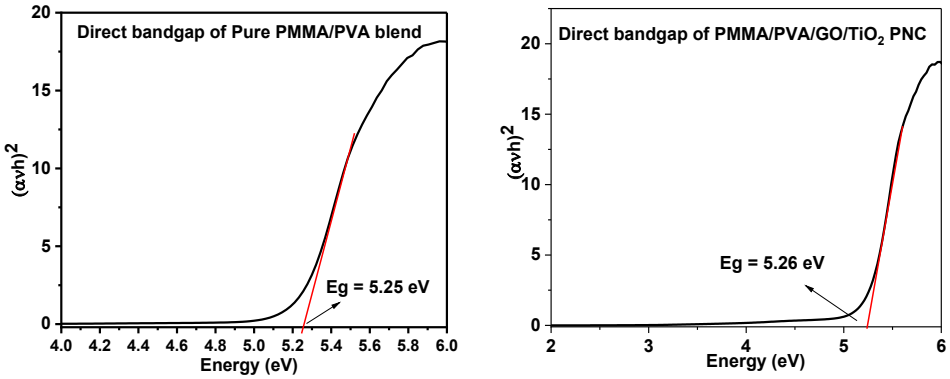

Fig. 5. Tauc's plots drawn for (a) Pure PMMA/PVA blend (b) PMMA-PVA-TiO_2-GO polymer nanocomposites

4. Conclusions

The newly developed PMMA-PVA-TiO_2-GO polymer nanocomposites have demonstrated noteworthy improvements in structural and optical properties due to the effective incorporation of TiO_2 and GO nanofillers into the host PMMA/PVA blend via a simple solution mixing method. XRD analysis have confirmed a reduction in crystallite size followed by increased micro-strain and dislocation density, indicating induced lattice distortions. These structural changes lead to improved mechanical performance, with higher Young's modulus and energy density with the reduced flexibility. Optical studies have revealed a red shift in the absorption edge along with improved absorption in UV region, while the optical bandgap remains nearly unchanged. Thus, the investigated nanocomposites can be suitable for advanced and flexible optoelectronics.

References

1. Alsaad, A. M., A. A. Ahmad, Abdul Raouf Al Dairy, Ayah S. Al-anbar, and Qais M. Al-Bataineh. "Spectroscopic characterization of optical and thermal properties of (PMMA-PVA) hybrid thin films doped with SiO_2 nanoparticles." *Results in Physics* 19 (2020): 103463. doi: 10.1016/j.rinp.2020.103463

2. Sa, Kadambinee, Prakash C. Mahakul, B. V. R. S. Subramanyam, Jagatpati Raiguru, Sonali Das, Injamul Alam, and Pitamber Mahanandia. "Effect of reduced graphene oxide-carbon nanotubes hybrid nanofillers in mechanical properties of polymer nanocomposites." In *IOP Conference Series: Materials Science and Engineering*, vol. 338, no. 1, p. 012055. IOP Publishing, 2018. doi: 10.1088/1757-899X/338/1/012055
3. Alsaad, Ahmad M., Ahmad A. Ahmad, Issam A. Qattan, Abdul-Raouf El-Ali, Shatha A. Al Fawares, and Qais M. Al-Bataineh. "Synthesis of optically tunable and thermally stable PMMA–PVA/CuO NPs hybrid nanocomposite thin films." *Polymers* 13, no. 11 (2021): 1715. doi: 10.3390/polym13111715
4. Sanes, José, Cristian Sánchez, Ramón Pamies, María-Dolores Avilés, and María-Dolores Bermúdez. "Extrusion of polymer nanocomposites with graphene and graphene derivative nanofillers: An overview of recent developments." *Materials* 13, no. 3 (2020): 549. doi: 10.3390/ma13030549
5. Liu, Shan, Shuhao Qin, Yue Jiang, Pingan Song, and Hao Wang. "Lightweight high-performance carbon-polymer nanocomposites for electromagnetic interference shielding." *Composites Part A: Applied Science and Manufacturing* 145 (2021): 106376. doi: 10.1016/j.compositesa.2021.106376
6. Sharma, Neha, Aakansha, M. G. Siddiqui, Saurabh Dalela, Shalendra Kumar, S. Z. Hashmi, M. Ayaz Ahmad, A. M. Quraishi, and P. A. Alvi. "Structural, optical, and electrical characteristics of synthesized novel and flexible PCCCe polymer nanocomposites for EMI shielding applications." *Journal of Applied Polymer Science* 142, no. 18 (2025): e56835. doi: 10.1002/app.56835
7. Losetty, Venkatramana, Sivarama Krishna Lakkaboyana, Hazarathaiah Yadav Chappidi, Katta Venkateswarlu, Herri Trilaksana, Janardhan Reddy Koduru, Ali Yuzir, Leonard I. Atanase, Praveen Kumar Seepana, and Salah Knani. "Transformative applications of polymer-based metal oxide nanocomposites in medicine, industry, and environmental remediation: a review." *Journal of Inorganic and Organometallic Polymers and Materials* 36, no. 1 (2026): 64-96. doi: 10.1007/s10904-025-03707-6
8. Sanchez, Clément, Beatriz Julián, Philippe Belleville, and Michael Popall. "Applications of hybrid organic–inorganic nanocomposites." *Journal of materials chemistry* 15, no. 35-36 (2005): 3559-3592. doi: 10.1039/B509097K
9. Loyalka, Swarnkesh, S. B. Dangi, S. Z. Hashmi, B. L. Choudhary, Saurabh Dalela, A. M. Quraishi, Shalendra Kumar, Aakansha, M. Ayaz Ahmad, and P. A. Alvi. "Improved functional properties of unique and novel PVDF/Ppy/ZnO (PPZ) polymer nanocomposites." *Composite Interfaces* (2025): 1-18. doi: 10.1080/09276440.2025.2546177
10. Badawi, Ali, and Sami S. Alharthi. "A comprehensive study of the linear/nonlinear optical and electrical features of rGO/Co: TiO_2 nanostructures incorporated PVP/PVA blend." *Journal of Inorganic and Organometallic Polymers and Materials* 34, no. 12 (2024): 5805-5816. doi: 10.1007/s10904-024-03215-z
11. Alonzo, Shanna Marie M., Moses Djanie Ashie, Gayani Pathiraja, and Bishnu Prasad Bastakoti. "A novel organic-inorganic hybrid polymerization strategy for

titanium oxide/polymer nanocomposites with supercapacitive properties." *Chemical Engineering Journal* 505 (2025): 159208. doi: 10.1016/j.cej.2025.159208

12. Dhayal, Vimala, S. Z. Hashmi, Upendra Kumar, B. L. Choudhary, A. E. Kuznetsov, Saurabh Dalela, Shalendra Kumar, Savas Kaya, S. N. Dolia, and P. A. Alvi. "Spectroscopic studies, molecular structure optimization and investigation of structural and electrical properties of novel and biodegradable Chitosan-GO polymer nanocomposites." *Journal of Materials Science* 55, no. 30 (2020): 14829-14847. doi: 10.1007/s10853-020-05093-5
13. Fadil, Yasemin, Le NM Dinh, Monique OY Yap, Rhiannon P. Kuchel, Yin Yao, Taro Omura, Ulises A. Aregueta-Robles et al. "Ambient-temperature waterborne polymer/rGO nanocomposite films: effect of rGO distribution on electrical conductivity." *ACS applied materials & interfaces* 11, no. 51 (2019): 48450-48458. doi: 10.1021/acsami.9b19183
14. Pandey, Gaurav, and Erik T. Thostenson. "Carbon nanotube-based multifunctional polymer nanocomposites." *Polymer Reviews* 52, no. 3 (2012): 355-416. doi: 10.1080/15583724.2012.703747
15. Masuda, Yoshitake, and Kazumi Kato. "Synthesis and phase transformation of TiO_2 nano-crystals in aqueous solutions." *Journal of the Ceramic Society of Japan* 117, no. 1363 (2009): 373-376. doi: 10.2109/jcersj2.117.373
16. Tauc, J. "Optical properties and electronic structure of amorphous Ge and Si". *Materials Research Bulletin*. (1968), **3**: 37–46. doi: 10.1016/0025-5408(68)90023-8
17. Sharma, Neha, Shalendra Kumar, Saurabh Dalela, S. Z. Hashmi, M. Ayaz Ahmad, Mohammed Ezzeldien, B. L. Choudhary, and P. A. Alvi. "Exploring and tailoring the characteristics of biocompatible next-generation soft materials: PCG and PCPtG polymer nanocomposites." *Diamond and Related Materials* (2026): 113454. doi: 10.1016/j.diamond.2026.113454
18. Tauc, J.; Grigorovici, R.; Vancu, A. "Optical Properties and Electronic Structure of Amorphous Germanium". *Physica Status Solidi B*. (1966) **15** (2): 627. doi: 10.1002/pssb.19660150224